

# Detrital zircon age constraints on the provenance of sandstones on Hatton Bank and Edoras Bank, NE Atlantic

Andrew C. Morton<sup>1,2</sup>, Kenneth Hitchen<sup>3</sup>, C. Mark Fanning<sup>4</sup>, Greg Yaxley<sup>4</sup>, Howard Johnson<sup>3</sup> and J. Derek Ritchie<sup>3</sup>

<sup>1</sup> HM Research Associates, 2 Clive Road, Balsall Common, West Midlands CV7 7DW, UK

<sup>2</sup> CASP, Department of Earth Sciences, University of Cambridge, 181a Huntingdon Road, Cambridge CB3 0DH, UK

<sup>3</sup> British Geological Survey, Murchison House, West Mains Road, Edinburgh EH9 3LA, UK

<sup>4</sup> Research School of Earth Sciences, The Australian National University, Canberra, ACT 0200, Australia

## ABSTRACT

U-Pb dating of detrital zircons shows that the provenance of Cretaceous-Palaeogene sandstones on Hatton and Edoras banks (SW Rockall Plateau) comprises magmatic rocks dated at c. 1800 Ma and c. 1750 Ma respectively. Their depositional setting, first-cycle mineralogy and unimodal nature detrital zircon populations suggest these sandstones are of local origin. The zircon age data are therefore considered to provide constraints on these poorly-understood areas of the Rockall Plateau. The U-Pb dates are directly comparable with U-Pb zircon crystallisation ages from granitoid rocks reported from the Ketilidian Belt of southern Greenland and from the Rhinns Complex of western Britain. Hf isotopic data from the Edoras Bank sample are consistent with derivation from a juvenile Palaeoproterozoic block. In conjunction with previously reported Sm-Nd  $T_{DM}$  model ages from the Ketilidian Belt, Rockall Bank and the Rhinns Complex, these data extend the known distribution of a large juvenile Palaeoproterozoic terrane spanning the southern NE Atlantic. By contrast, Hf isotopic data from the Hatton Bank sample imply a large contribution from Archaean crust. The zircon population from Edoras Bank also contains sparse Mesoproterozoic grains, providing evidence for the presence of volumetrically minor Grenville-age intrusions in the southern part of the Rockall Plateau.

Keywords: provenance, zircon dating, Hf isotopes, Rockall, Cretaceous, Palaeogene

## INTRODUCTION

The Rockall Plateau (Fig. 1) is a submerged continental crustal block separated from the northern European continental margin by the highly attenuated crust underlying the Rockall Trough, and from Greenland by oceanic crust (Roberts, 1975; Roberts et al., 1988; Joppen and White, 1990; Hitchen, 2004). The area occupies a critical location in pre-drift North Atlantic reconstructions, but because of the scarcity of samples, the geological history of the basement is poorly understood. The only direct evidence for the nature of the basement forming the Rockall Plateau comes from samples acquired from Rockall Bank. Sm-Nd model ( $T_{DM}$ ) ages for five samples (A to E, Fig. 1) recovered during diving expeditions (Roberts et al., 1973) range from 1.89-2.14 Ga (Morton and Taylor 1991). A similar  $T_{DM}$  age (1.91 Ga) has been reported more recently from two further sites (56-15/11 and 56-15/12, Fig. 1) in the area (Hitchen, 2004). Although no U-Pb zircon age data from these samples have been formally published, Daly et al. (1995) and Scanlon and Daly (2001) indicate that single-grain zircon age dating of samples A, C and D (Fig. 1) yielded results similar to that of the Annagh Gneiss of north Mayo (Ireland), which has a U-Pb zircon crystallisation age of c. 1750 Ma. These limited data suggest that the Rockall Bank metamorphic basement comprises a juvenile Palaeoproterozoic terrane (Morton and Taylor 1991; Dickin, 1992).

No basement rocks have been recovered from the other bathymetric highs (Hatton, Edoras and George Bligh banks) that comprise the Rockall Plateau (Fig. 1). Palaeogene basalts from George Bligh Bank display evidence of contamination by Archaean crust (Hitchen et al., 1997), suggesting that the boundary between the Archaean and Palaeoproterozoic terranes lies between Rockall Bank and George Bligh Bank, as proposed by Dickin (1992) and Dickin and Durant (2002). Pb isotopic evidence for Proterozoic contamination of Blackstones Bank basaltic rocks led Dickin and Durant (2002) to place the boundary to the north of this Tertiary igneous complex. Likewise, the boundary between the Archaean and Palaeoproterozoic terranes lies to the north of Stanton Bank (Fig. 1), a submerged bathymetric high, on the basis of the occurrence of basement rocks with relatively young Sm-Nd  $T_{DM}$  model ages (Scanlon et al., 2003). The location of the proposed boundary coincides with the central strand of the Anton Dohrn lineament as defined from potential field data by Kimbell et al. (2005). Although the location of the boundary west of George Bligh and Rockall banks is not directly constrained from any geological sample data, the central strand of the Anton Dohrn Lineament crosses Hatton Bank at a marked inflection point of the axial trace of the North Hatton Bank Anticline (Johnson et al., 2005). To date, there is no evidence, either direct or indirect, regarding the basement underlying Hatton and Edoras banks, which are located in the southwestern part of the Rockall Plateau, separated from Rockall Bank by the intervening Hatton Basin (Fig. 1).

In this paper, we present the results of a combined U-Pb and Lu-Hf isotopic study of detrital zircons from Cretaceous-Palaeogene sandstones recovered by coring at two sites, one on Hatton Bank (BGS borehole 99/2A) and one close to Edoras Bank (DSDP Site 555), and discuss their implications regarding the age of the basement underlying these two poorly understood areas.

## ANALYTICAL METHODS

Zircon concentrates were obtained using standard density and magnetic separation techniques. Arbitrary, and presumed representative, fractions were poured onto double sided tape, cast into an epoxy resin disk, sectioned and polished. Transmitted and reflected light photomicrographs, together with cathodoluminescence (CL) images, were prepared for all grains. Representative transmitted light photomicrographs for the two samples are shown in Fig. 2.

The U-Pb analyses were undertaken using SHRIMP RG at The Australian National University in Canberra. The procedures employed for zircon U-Pb dating followed Williams (1998) and references therein. The number of scans through the mass stations was limited to four, thereby achieving rapid data acquisition at the expense of some counting precision per analysis. An arbitrary group of 60 zircons were analysed from each sample. Subjectivity in zircon dating was avoided by analysing all zircons encountered during the traverse of the mount, unless the grain showed evidence of being metamict or otherwise structurally compromised, as determined by examination of the reflected and transmitted light photomicrographs and CL images. Normalisation of Pb/U isotopic ratios was achieved by reference to analyses of the FC1 reference zircon (1099 Ma:  $^{206}\text{Pb}/^{238}\text{U} = 0.1589$ ; Paces and Miller, 1993). The raw SHRIMP data were processed using SQUID (Ludwig, 2000), with plots generated using Isoplot/Ex (Ludwig, 1999). The measured  $^{206}\text{Pb}/^{204}\text{Pb}$  ratios have been used to correct for common Pb and the radiogenic  $^{207}\text{Pb}/^{206}\text{Pb}$  ratio has been used to calculate the preferred age, despite the fact that a number of the areas analysed are interpreted to have lost radiogenic Pb. The zircon age data are presented in Tables 1 and 2.

Hf isotopic analyses were performed by laser ablation on the same locations as previously analysed by SHRIMP, using the reflected light micrographs to reveal the locations of the ion probe sputter pits (typically about 30  $\mu\text{m}$  across). For most analyses of unknowns or secondary standards, the laser spot size on the sample was either 47 or 37  $\mu\text{m}$  in diameter, depending on the size of the grain and the nature of internal structure as revealed by cathodoluminescence imaging.

The Hf isotope measurements were conducted by laser ablation multicollector inductively coupled plasma mass spectroscopy using the RSES Neptune MC-ICPMS coupled to a 193 nm ArF Excimer laser. The mass spectrometer was first tuned to optimal sensitivity using a large grain of zircon from the Monastery kimberlite. All isotopes were measured simultaneously in static-collection mode. A gas blank was acquired at regular intervals throughout the analytical session (every 10 or so analyses). The laser was fired with typically 5-8Hz repetition rate and 60 mJ energy. Data were acquired for 100 seconds, but in many cases only a selected interval from the total acquisition was used in data reduction. In each batch of samples between gas blank measurements, several secondary standard zircons (91500, FC-1, Temora-2, Monastery and Mud Tank) were measured as a check on data quality, along with several unknowns. Signal intensity was typically  $\approx 5-6$  V for total Hf at the beginning of ablation, and decreased over the acquisition time to 2 V or less. The Hf isotopic data are presented in Table 3.

### **BOREHOLE 99/2A**

BGS borehole 99/2A was drilled into the Mesozoic succession on Hatton Bank (Hitchen, 2004), and recovered 28.5 m of sandstone and siltstone dated as Albian on the basis of terrestrial palynomorphs. The sample selected for zircon isotopic analysis was taken from 45.65-45.72 m within the Albian clastic succession. The absence of marine microplankton and low overall species diversity indicates a paralic depositional environment. The sandstone is dominated by fresh angular quartz and feldspar, and contains a heavy mineral assemblage dominated by unstable phases such as calcic amphibole and epidote (Hitchen, 2004). These characteristics suggest first-cycle derivation from basement of intermediate-acidic aspect. The zircon morphologies (Fig. 2) provide further support for first-cycle derivation, with all grains having euhedral or angular habits. In transmitted light, the zircons show evidence for structural imperfections, with large cracks evident in many grains. Cathodoluminescence images of the zircons (Fig. 2) show that they have typical magmatic zoning patterns (Corfu et al., 2003). Grains with apparent cores form a small proportion of the zircon population, but where they do occur (e.g. grain 13) they have similar ages to rims on other grains with cores (e.g. grains 4 and 6). Hence, although some zircons are structured (in that they have cores and rims), there is little to no apparent age difference. This is not uncommon in zoned igneous zircons. Although there are discontinuities in zoning between apparent centres and rims, the lack of a significant age difference, at least at the uncertainties of our measurements, implies either that the chemistry of the magma changed during crystallisation, or that there were two or more other magmatic pulses within a short period of time.

The U-Pb isotopic data and ages of individual grains are given in Table 1. All the zircons in the sample have relatively high Th/U, indicating they have an igneous parentage, probably of felsic-intermediate composition (Hartmann and Santos, 2004; Link et al., 2005). Many of the grains are significantly discordant, with the U-Pb isotopic data defining a simple discordia line with a lower intercept within uncertainty of the present day. This suggests that the isotopic system has been disturbed by a present-day event. However, fission track analysis and (U-Th)/He dating of apatites identified a thermal event with a maximum palaeo-temperature of 50°C and subsequent cooling beginning around 80-50 Ma (Hitchen, 2004). This was interpreted as the result of the Late Palaeocene-Early Eocene magmatic event associated with the opening of this sector of the NE Atlantic. In view of this, a linear regression with a lower intercept at 55 Ma was forced through the data (Fig. 3). Although this alternative regression line is not as well fitted (MSWD of 1.4, compared with 1.2), it appears more geologically plausible.

Despite the discordance shown by many grains, the combined histogram - relative probability plot indicates that the zircons form a single coherent population of  $^{207}\text{Pb}/^{206}\text{Pb}$  ages (Fig. 4). The only zircons that deviate from this population are highly discordant, and their ages are therefore unreliable. The single peak has a mean  $^{207}\text{Pb}/^{206}\text{Pb}$  age of  $1798.5 \pm 4.5$  Ma (MSWD 0.69). This calculation used the entire zircon population, with only three zircons (grains 4.1, 24.1 and 31.1) falling outside error, all of which are highly discordant (35%, 79% and 43% respectively).

$\epsilon\text{Hf}(t)$  values for the zircons from borehole 99/2A range from +2.97 to -3.30 (Table 3, Fig. 5), with  $T_{\text{DM}}$  ages ranging from 2216-2643 Ma. These  $\epsilon\text{Hf}(t)$  values differ significantly from that estimated for the depleted mantle at c. 1800 Ma (Vervoort and Blichert-Toft, 1999). The Hf isotopic data therefore indicate that the depleted mantle was not entirely responsible for generating the magmas from which the zircons crystallised, and that a large proportion of pre-existing crust of Archaean age must have been involved.

## **SITE 555**

DSDP Site 555 is located on a col between Edoras Bank and Hatton Bank, to the SW of BGS borehole 99/2A (Fig. 1). Beneath a Miocene deep water biogenic pelagic succession, the borehole encountered a Palaeocene-Eocene succession dominated by basalt flows and volcanoclastic sediment, with occasional units containing terrigenous clastic sediments (Shipboard Scientific Party, 1984). This volcanic-dominated succession was generated during the early stages of seafloor spreading between Rockall Plateau and Greenland, and is coeval

with the seaward dipping reflector sequence found to the SW of Edoras Bank (Roberts et al., 1984).

The sample analysed by SHRIMP (555-88-5, 18-25 cm) is a feldspathic and micaceous sandstone from subunit IVb, dated as Late Palaeocene on the basis of nannofossils and dinoflagellates (Shipboard Scientific Party, 1984). Sedimentary structures in this subunit include scours, cross-lamination and soft sediment deformation, suggesting a high-energy depositional environment. This, taken in conjunction with the microfossil evidence, argues for deposition in a nearshore marine environment. There are strong volcanic influences throughout the subunit, including interbedded thin basalt flows and abundant tuffs and lapilli tuffs. Heavy minerals assemblages are rich in apatite and garnet, with subordinate zircon, epidote and amphibole (Morton, 1984), indicating derivation from basement of predominantly intermediate-acidic aspect. The zircon habits (Fig. 2) are strongly suggestive of a first-cycle origin, with grains lacking significant degrees of rounding. The transmitted light photomicrographs show that the grains from DSDP Site 555 are much simpler and less structured, with more large clear areas that could be analysed, compared with grains from borehole 99/2A, which show more zoning and cracking (Fig. 2). Cathodoluminescence images of the zircons (Fig. 2) show that they have typical magmatic zoning patterns (Corfu et al., 2003). Grains with apparent cores are present in small numbers.

The analysed zircons in the sample from Site 555 are concordant or near-concordant, with only one zircon being more than 20% discordant (Fig. 3). The zircon age spectrum is slightly more diverse than in borehole 99/2A, although the vast majority of the zircons (c. 80%) comprise a single  $^{207}\text{Pb}/^{206}\text{Pb}$  peak (Fig. 4) with a weighted mean age of  $1749.5 \pm 2.7$  Ma (MSWD 0.79 for 47 analyses). The significance of the other  $^{207}\text{Pb}/^{206}\text{Pb}$  ages is uncertain, since they do not form a coherent group. There is a single very early Palaeoproterozoic grain with a large error bar ( $2477 \pm 68$  Ma), a discordant grain dated as  $1971 \pm 89$  Ma, a small number of grains slightly younger than the main peak (ranging down to 1605 Ma), and two late Mesoproterozoic grains (1003 Ma, 1112 Ma). As with the sample from borehole 99/2A, all the zircons in the sample have relatively high Th/U, implying an igneous parentage of felsic-intermediate composition.

The Hf isotopic data contrast markedly with those from borehole 99/2A (Table 3, Fig. 5), with  $\epsilon\text{Hf}_{(t)}$  values ranging from +1.86 to +6.49 (excluding one zircon with an  $\epsilon\text{Hf}_{(t)}$  value of -1.86). These values correspond to  $T_{\text{DM}}$  ages of 1964-2266 Ma, with one outlier at 2491 Ma. The depleted mantle was therefore a major contributor to the magmas from which these zircons crystallised, although there is some evidence for the involvement of pre-existing crust.

## DISCUSSION

The zircon age distributions in the Edoras and Hatton Bank samples indicate that the sediment was derived almost exclusively from basement rocks dated as c. 1750 Ma and c. 1800 Ma respectively. There are several lines of evidence indicating that the sediment was locally derived. The succession cored in borehole 99/2A was deposited in a non-marine environment and is characterised by first-cycle sediment, suggesting local derivation from adjacent basement on Hatton Bank. Subunit IVb at Site 555 was deposited in a high-energy nearshore environment, again suggesting proximity to the hinterland, and contains heavy mineral assemblages of first-cycle aspect. Regional variations in heavy mineral assemblages on the SW Rockall Plateau margin indicate the sandstones in this part of the Site 555 succession were derived from the Rockall Plateau, rather than from the conjugate SE Greenland margin (Morton, 1984).

Link et al. (2005) recently conducted a study of detrital zircon age distributions in 1<sup>st</sup> and 2<sup>nd</sup> order drainage systems as defined by Ingersoll (1990) and Ingersoll et al. (1993). They showed that 1<sup>st</sup> order systems, which range from talus slopes to small fluvial drainages, contain 'defining grain populations' that form over 50% of the entire zircon distribution. These defining populations are also seen in 2<sup>nd</sup> order systems, but in lower abundances due to dilution by sediment introduced by other tributaries. The two zircon assemblages described in this paper are both dominated by single 'defining grain populations', their age distributions being characterised by single peaks comprising 100% of the zircons in borehole 99/2A and 80% of the zircons in Site 555. The zircon age data therefore suggest that the sandstones at the two locations are of local origin, since they represent the products of small-scale 1<sup>st</sup> order drainage systems.

The only plausible alternative provenance for the zircons in the samples from borehole 99/2A and Site 555 would be the Ketilidian Belt of southern Greenland, which was adjacent to Hatton and Edoras banks prior to opening of the NE Atlantic (Fig. 6). Derivation from the east (Rockall Bank) can be ruled out since the intervening Hatton Basin was a depocentre during the Mesozoic and Cenozoic (Hitchen, 2004). The ages found in borehole 99/2A and Site 555 (c. 1800 Ma and c. 1750 Ma respectively) fall within the range shown by granitoids of the Ketilidian Belt (c. 1850 Ma to c. 1730 Ma; Garde et al., 2002). However, if the sediment had been derived from the Ketilidian Belt, individual samples would be expected to show a wider range of zircon ages than is actually observed, given the 120 Ma age range present in the Ketilidian catchment (Fig. 6). Therefore, on the basis of depositional

environment and zircon age distributions, the zircons in borehole 99/2A and Site 555 are considered to be locally derived, rather than transported from the conjugate margin in southern Greenland. Consequently, they are believed to be representative of local basement on Edoras and Hatton banks.

This provenance study therefore provides evidence for the existence of basement rocks dated as c. 1750 Ma on Edoras Bank and c. 1800 Ma on Hatton Bank. The Hatton and Edoras basement appears to be closely comparable to that of Rockall Bank, since single-grain zircon age dating on samples A, C and D (Fig. 6) yielded results similar to that of the Annagh Gneiss of north Mayo (Ireland), which has a U-Pb zircon crystallisation age of c. 1750 Ma (Daly et al., 1995; Scanlon and Daly, 2001).

Dickin (1992) showed a reconstruction of the southern NE Atlantic, drawing attention to the similarity in Sm-Nd  $T_{DM}$  ages between the Rockall Bank ( $T_{DM} = 1.89-2.14$ ), the Ketilidian Belt of southern Greenland ( $T_{DM} = 1.98-2.18$  Ga) and the Rhinns Complex of Ireland and western Scotland ( $T_{DM} = 1.91-1.98$  Ga). On the basis of the Sm-Nd isotopic data, he suggested these areas originally comprised a single juvenile Palaeoproterozoic crustal province.

The Ketilidian Belt of southern Greenland, which, on a continental reconstruction, abuts the western margin of the Rockall Plateau (Fig. 6), is characterised by two main phases of granitoid emplacement (Garde et al., 2002). The first phase comprises intrusion of the calc-alkaline Julienehåb batholith at 1854-1795 Ma, closely followed by high temperature-low pressure metamorphism and intrusion of I-type granites at 1795-1785 Ma. A second phase comprising emplacement of rapakivi granite sheets occurred at 1755-1732 Ma. The U-Pb dates acquired from the two samples from Hatton and Edoras banks can be directly matched with the two phases of granite emplacement in the Ketilidian Belt. The c. 1750 Ma date from Edoras Bank matches the age of the rapakivi granites, and the c. 1800 Ma date from Hatton Bank matches the earlier phase.

The Rhinns Complex, which lies to the east of the Rockall Plateau (Fig. 6), comprises basement rocks that outcrop on Islay and Colonsay in southwest Scotland, and on Inishtrahull and Tor Rocks in northwest Ireland (Muir et al., 1994). Gneisses from Islay have  $T_{DM}$  ages of 1.93-1.98 Ga and a U-Pb zircon crystallisation age of c. 1780 Ma (Marcantonio et al., 1988), closely comparable to gneisses from Inishtrahull, which have  $T_{DM}$  ages of 1.91-1.98 Ga and a U-Pb zircon crystallisation age of c. 1780 Ma (Daly et al., 1991). The Rhinns Complex therefore represents juvenile Palaeoproterozoic crust with similar characteristics to Rockall Bank and the Ketilidian Belt.

The new U-Pb age data from Edoras and Hatton banks therefore provide a link between the Ketilidian Belt to the southwest, Rockall Bank to the east, and the Rhinns Complex to the northeast, and support the concept of a juvenile Palaeoproterozoic block across the southern part of the NE Atlantic. However, the Hf isotopic data introduce a degree of complexity to this apparently simple picture. The results from Edoras Bank ( $\epsilon\text{Hf}_{(t)}$  values ranging from +1.86 to +6.49,  $T_{\text{DM}}$  ages ranging from 1964-2266 Ma) are consistent with the derivation from a juvenile Palaeoproterozoic block. The  $\epsilon\text{Hf}_{(t)}$  values from the Edoras Bank sample are consistent with  $\epsilon\text{Nd}_{(t)}$  values reported from the Ketilidian Belt, where metatholeiites have  $\epsilon\text{Nd}_{(t)}$  between -5 and +5, granitoids have  $\epsilon\text{Nd}_{(t)}$  between -0.6 and +1.6, and norites have  $\epsilon\text{Nd}_{(t)}$  between +0.4 and +2.8 (Patchett and Bridgwater, 1984; Brown et al., 2003). Following Vervoort and Blichert-Toft (1999), these  $\epsilon\text{Nd}_{(t)}$  values are approximately equivalent to  $\epsilon\text{Hf}_{(t)}$  values of between +7.7 and +9.1 for the metatholeiites, between +1.3 and +4.3 for the granitoids, and between +2.1 and +3.5 for the norites. The Nd isotopic data from the Ketilidian Belt have been interpreted as showing that the metatholeiites represent a juvenile mantle contribution, and that the granitoids represent juvenile mantle with a c. 10% contribution from Archaean crust, the latter comprising clastic material that had been transported to the orogenic zone and deposited on oceanic crust (Patchett and Bridgwater, 1984).

By contrast, the results from borehole 99/2A indicate that the magmatic source that supplied the zircons to the Hatton Bank site had a large Archaean component ( $\epsilon\text{Hf}_{(t)}$  values ranging from +2.97 to -3.30,  $T_{\text{DM}}$  ages ranging from 2216 to 2643 Ma). According to the geophysical evidence, borehole 99/2A lies a considerable distance (approximately 230 km) from the proposed Archaean-Palaeoproterozoic boundary, and on pre-drift reconstructions (Fig. 6), Hatton Bank abuts the Ketilidian Belt of southern Greenland. The presence of a large Archaean component is therefore surprising. In the Border Zone of the Ketilidian Belt (the c. 50 km wide zone that lies between the Juliehåb batholith and the North Atlantic Craton), there is isotopic evidence for extensive Archaean contamination of Ketilidian-age granitoids (Kalsbeek and Taylor, 1985), but this disappears rapidly southwards. The combination of a c. 1800 Ma zircon U-Pb crystallisation age and a large Archaean Hf component is consistent with derivation from a granitoid with similar characteristics to those of the Border Zone in the Ketilidian Belt, but given the distance from the proposed boundary and the relatively narrow width of the Border Zone, this would require relatively long distance transport, a possibility that seems unlikely given the depositional setting and the unimodal nature of the detrital zircon population. There are a number of other possible explanations for the anomaly: for example, the interpreted location of the Palaeoproterozoic-Archaean boundary at the northern end of Hatton Bank may be incorrect, or the melt that generated the Hatton Bank

igneous body included a large proportion of Archaean-derived sediment. Perhaps more likely is that the distribution of Archaean and Palaeoproterozoic crust is more complex than currently envisaged, especially in view of the recently-published evidence for the presence of suspect terranes comprising Palaeoproterozoic juvenile crust within the Lewisian (Kinny et al., 2005). Finally, Dahl-Jensen et al. (1998) interpreted seismic profiles from southern Greenland as showing the presence of an Archaean wedge in the lower crust beneath the Juliehåb batholith, a model that would suggest the batholith was emplaced through Archaean crust (Garde et al., 2002). By analogy, it is possible that there is a relatively thick wedge of Archaean crust at depth below Hatton Bank. In the absence of direct basement samples from the area, none of these possibilities can be definitively ruled in or out.

The zircon age data from Hatton and Edoras banks suggest that, following the creation of the Palaeoproterozoic crustal block, the area remained comparatively undisturbed by tectonothermal events until rifting took place during the Mesozoic and Palaeocene, leading to continental break-up and subsequent seafloor spreading in the Early Eocene. However, the data may have some significance regarding the location of the Grenville Front. Miller et al. (1973) reported a whole-rock Ar-Ar age of c. 1.0 Ga for sample B (Fig. 1) from Rockall Bank, suggesting that the Grenville Front may have passed across the southern part of the Rockall Plateau. The Ketilidian Belt includes minor younger intrusions, such as the Paatusoq syenite, dated at c. 1140 Ma (Grocott et al., 1999). The presence of two Mesoproterozoic zircon grains (c. 1005 Ma and c. 1110 Ma) in the sample from Site 555 suggests that similar, but volumetrically-minor, broadly Grenville-age intrusions may be present in the southern part of the Rockall Plateau.

## ACKNOWLEDGEMENTS

We are grateful to Stephen Daly, Paul Link and Martin Whitehouse for their constructive comments on this manuscript, and to Sheila Jones for drafting Figures 1 and 6. KH, HJ and JDR publish with permission of the Executive Director, British Geological Survey (NERC).

## REFERENCES

- Blichert-Toft, J. and Albarède, F. 1997. The Lu–Hf isotope geochemistry of chondrites and the evolution of the mantle–crust system. *Earth and Planetary Science Letters*, **148**, 243–258.
- Brown, P.E., Dempster, T.J., Hutton, D.H.W. and Becker, S.M. 2003. Extensional tectonics and mafic plutons in the Ketilidian rapakivi granite suite of South Greenland. *Lithos*, **67**, 1–13.

- Cole, J.E. and Peachey, J. 1999. Evidence for pre-Cretaceous rifting in the Rockall Trough: analysis using quantitative plate tectonic modelling. *In: Fleet, A.J. and Boldy, S.A.R. (eds) Petroleum Geology of Northwest Europe: Proceedings of the 5<sup>th</sup> Conference.* Geological Society, London. 359-370.
- Corfu, F., Hanchar, J.M., Hoskin, P.W.O. and Kinny, P. 2003. Atlas of zircon textures. *In: Hanchar, J.M. and Hoskin, P.W.O. (eds) Zircon. Reviews in Mineralogy and Geochemistry, 55*, 469-500.
- Dahl-Jensen, T., Thybo, H., Hopper, J. and Rosing, M. 1998. Crustal structure at the SE Greenland margin from wide-angle and normal incidence seismic data. *Tectonophysics, 288*, 191-198.
- Daly, J.S., Muir, R.J. and Cliff, R.A. 1991. A precise U-Pb age of the Inishtrahull syenitic gneiss, County Donegal, Ireland. *Journal of the Geological Society, London, 148*, 639-642.
- Daly, J.S., Heaman, L.M., Fitzgerald, R.C., Menuge, J.F., Brewer, T.S., and Morton, A.C. 1995. Age and crustal evolution of crystalline basement in western Ireland and Rockall. *In: Croker, P.F. & Shannon, P.M. (eds) The Petroleum Geology of Ireland's Offshore Basins.* Geological Society of London, Special Publications, **93**, 433-434.
- Dickin, A.P. 1992. Evidence for an Early Proterozoic crustal province in the North Atlantic region. *Journal of the Geological Society, London, 149*, 483-486.
- Dickin, A.P. and Durant, G.P. 2002. The Blackstones Bank igneous complex: geochemistry and crustal context of a submerged Tertiary igneous centre in the Scottish Hebrides. *Geological Magazine, 139*, 199-207.
- Garde, A.A., Hamilton, M.A., Chadwick, B., Grocott, J. and McCaffrey, K.J.W. 2002. The Ketilidian orogen of South Greenland: geochronology, tectonics, magmatism, and fore-arc accretion during Palaeoproterozoic oblique convergence. *Canadian Journal of Earth Sciences, 39*, 765-793.
- Goodge, J.W. and Vervoort, J.D. 2006. Origin of Mesoproterozoic A-type granites in Laurentia: Hf isotope evidence. *Earth and Planetary Science Letters, 243*, 711-731.
- Grocott, J., Garde, A.A., Chadwick, B., Cruden, A.R. and Swager, C. 1999. Emplacement of rapakivi granite and syenite by floor depression and roof uplift in the Palaeoproterozoic Ketilidian orogen, South Greenland. *Journal of the Geological Society, London, 156*, 15-24.
- Hartmann, L.A. and Santos, J.O.S. 2004. Predominance of high Th/U, magmatic zircon in Brazilian Shield sandstones. *Geology, 32*, 73-76.
- Hitchen, K. 2004. The geology of the UK Hatton-Rockall margin. *Marine and Petroleum Geology, 21*, 993-1012.
- Hitchen, K., Morton, A.C., Mearns, E.W., Whitehouse, M. and Stoker, M.S. 1997. Geological implications from geochemical and isotopic studies of Late Cretaceous and early Tertiary igneous rocks around the northern Rockall Trough. *Journal of the Geological Society, London, 154*, 517-521.

Ingersoll, R.V. 1990. Actualistic sandstone petrofacies: discriminating modern and ancient source rocks. *Geology*, **18**, 733-736.

Ingersoll, R.V., Kretchmer, A.G. and Valles, P.K. 1992. The effect of sampling scale on actualistic sandstone petrofacies. *Sedimentology*, **40**, 937-953.

Johnson, H., Ritchie, J.D., Hitchen, K., McInroy, D.B. and Kimbell, G.S. 2005. Aspects of the Cenozoic deformational history of the northeast Faroe-Shetland Basin, Wyville-Thomson Ridge and Hatton Bank areas. In: Doré, A.G. and Vining, B. (eds) *Petroleum Geology: North-West Europe and Global perspectives: Proceedings of the 6<sup>th</sup> Petroleum Geology Conference*. Geological Society, London, 993-1007.

Joppen, M. and White, R.S. 1990. The structure and subsidence of Rockall Trough from two-ship seismic experiments. *Journal of Geophysical Research*, **95**, 19821-19837.

Kalsbeek, F. and Taylor, P.N. 1985. Isotopic and chemical variation in granites across a Proterozoic continental margin – the Ketilidian mobile belt of South Greenland. *Earth and Planetary Science Letters*, **73**, 65-80.

Kimbell, G.S., Ritchie, J.D., Johnson, H. and Gatliff, R.W. 2005. Controls on the structure and evolution of the NE Atlantic margin revealed by regional potential field imaging and 3D modelling. In: Doré, A.G. and Vining, B. (eds) *Petroleum Geology: North-West Europe and Global perspectives: Proceedings of the 6<sup>th</sup> Petroleum Geology Conference*. Geological Society, London, 933-945.

Kinny, P.D., Friend, C.R.L. and Love, G.J. 2005. Proposal for a terrane-based nomenclature for the Lewisian Gneiss Complex of NW Scotland. *Journal of the Geological Society, London*, **162**, 175-186.

Link, P.K., Fanning, C.M. and Beranek, L.P. 2005. Reliability and longitudinal change of detrital zircon-age data in the Snake River system, Idaho and Wyoming: an example of reproducing the bumpy barcode. *Sedimentary Geology*, **182**, 101-142.

Ludwig, K.R. 1999. *User's manual for Isoplot/Ex, version 2.10, a geochronological toolkit for Microsoft Excel*. Berkeley Geochronology Center, Special Publication, **1a**.

Ludwig, K.R. 2000. *SQUID 1.00, a user's manual*. Berkeley Geochronology Center, Special Publication, **2**.

Marcantonio, F., Dickin, A.P., McNutt, R.H. and Heaman, L.M. 1988. A 1800-million-year-old Proterozoic gneiss terrane in Islay with implications for the crustal structure and evolution of Britain. *Nature*, **335**, 620-624.

Miller, J.A., Matthews, D.H. and Roberts, D.G. 1973. Rock of Grenville age from Rockall Bank. *Nature, Physical Science*, **246**, 61.

Morton, A.C. 1984. Heavy minerals from Paleogene sediments, Deep Sea Drilling Project Leg 81: their bearing on stratigraphy, sediment provenance and the evolution of the North

Atlantic. In: Roberts, D.G., Schnitker, D., et al. *Initial Reports of the Deep Sea Drilling Project*, **81**. U.S. Government Printing Office, Washington, 653-661.

Morton, A.C. and Taylor P.N. 1991. Geochemical and isotopic constraints on the nature and age of basement rocks from Rockall Bank, NE Atlantic. *Journal of the Geological Society, London*, **147**, 631-634.

Muir, R.J., Fitches, W.J., Maltman, A.J. and Bentley, M.R. 1994. Precambrian rocks of the southern Inner Hebrides-Malin Sea region: Colonsay, west Islay, Inishtrahull and Iona. In: Gibbons, W.S. and Harris, A.L. (eds) *A revised correlation of Precambrian rocks of the British Isles*. Geological Society, London, Special Report, **22**, 54-58.

Paces, J. B. and Miller, J. D. 1993. Precise U-Pb ages of Duluth Complex and related mafic intrusions, northeastern Minnesota: geochronological insights to physical, petrogenetic, paleomagnetic, and tectonomagmatic process associated with the 1.1 Ga Midcontinent Rift System. *Journal of Geophysical Research*, **98**, 13997-14013.

Patchett, J.P. and Bridgwater, D. 1984. Origin of continental crust of 1.9-1.7 Ga age defined by Nd isotopes in the Ketilidian terrain of South Greenland. *Contributions to Mineralogy and Petrology*, **87**, 311-318.

Roberts, D.G. 1975. Marine geology of the Rockall Plateau and Trough. *Philosophical Transactions of the Royal Society of London*, **278**, 447-509.

Roberts, D.G., Ardu, D.A. and Dearnley, R. 1973. Precambrian rocks drilled on Rockall Bank. *Nature, Physical Science*, **244**, 21-23.

Roberts, D.G., Backman, J., Morton, A.C., Murray, J.W. and Keene, J.B. 1984. Evolution of volcanic rifted margins: synthesis of Leg 81 results on the west margin of Rockall Plateau. In: Roberts, D.G., Schnitker, D., et al. *Initial Reports of the Deep Sea Drilling Project*, **81**. U.S. Government Printing Office, Washington, 883-911.

Roberts, D.G., Ginzburg, A., Nunn, K. and McQuillin, R. 1988. The structure of the Rockall Trough from seismic refraction and wide-angle reflection measurements. *Nature*, **332**, 632-635.

Scanlon, R. and Daly, J.S. 2001. Basement architecture of the rifted Northeast Atlantic margin: evidence from a combined geochronology, fission-track and potential field study. *Geological Society of America Annual Meeting, Boston, Massachusetts, Abstracts with Programs*, paper 64-0.

Scanlon, R.P., Daly, J.S. and Whitehouse, M.J. 2003. The c. 1.8 Ga Stanton Banks Terrane, offshore Western Scotland, a large juvenile Palaeoproterozoic crustal block within the accretionary Lewisian complex. *Geophysical Research Abstracts*, **5**, 13248.

Shipboard Scientific Party 1984. Site 555. In: Roberts, D.G., Schnitker, D., et al. *Initial Reports of the Deep Sea Drilling Project*, **81**. U.S. Government Printing Office, Washington, 277-399.

Söderlund, U., Patchett, P.J., Vervoort, J.D. and Isachsen, C.E. 2004. The  $^{176}\text{Lu}$  decay constant determined by Lu-Hf and U-Pb systematics of Precambrian mafic intrusions. *Earth and Planetary Science Letters*, **219**, 311-324.

Vervoort, J.D. and Blichert-Toft, J. 1999. Evolution of the depleted mantle: Hf isotope evidence from juvenile rocks through time. *Geochimica et Cosmochimica Acta*, **63**, 533-556.

Williams, I.S. 1998. U-Th-Pb geochronology by ion microprobe. In: McKibben, M.A., Shanks, W.C. III and Ridley, W.I. (eds) *Applications of microanalytical techniques to understanding mineralising processes*. Society of Economic Geologists, Reviews in Economic Geology, **7**, 1-35.

**TABLE CAPTIONS**

Table 1. Summary of SHRIMP U-Pb zircon results for BGS borehole 99/2A, 45.65-45.72 m (Hatton Bank). Uncertainties given at the one  $\sigma$  level. Error in FC1 Reference zircon calibration was 0.37% for the analytical session (not included in above errors but required when comparing  $^{206}\text{Pb}/^{238}\text{U}$  data from different mounts).  $f_{206}$  % denotes the percentage of  $^{206}\text{Pb}$  that is common Pb. Correction for common Pb made using the measured  $^{204}\text{Pb}/^{206}\text{Pb}$  ratio. For % Disc, 0% denotes a concordant analysis.

Table 2. Summary of SHRIMP U-Pb zircon results for DSDP sample 555-88-5, 18-25 cm (Edoras Bank). Uncertainties given at the one  $\sigma$  level. Error in FC1 Reference zircon calibration was 0.37% for the analytical session (not included in above errors but required when comparing  $^{206}\text{Pb}/^{238}\text{U}$  data from different mounts).  $f_{206}$  % denotes the percentage of  $^{206}\text{Pb}$  that is common Pb. Correction for common Pb made using the measured  $^{204}\text{Pb}/^{206}\text{Pb}$  ratio. For % Disc, 0% denotes a concordant analysis.

Table 3. Hf isotopic compositions of detrital zircons from BGS borehole 99/2A and DSDP Site 555.  $^{176}\text{Lu}$  decay constant from Söderlund et al. (2004). Chondritic values from Blichert-Toft and Albarède (1997). Present day depleted mantle values from Vervoort and Blichert-Toft (1999). “Bulk Earth” from Goodge and Vervoort (2006).

## FIGURE CAPTIONS

Fig. 1. Location of the Rockall Plateau west of Britain, showing the main bathymetric features and location of sites discussed in the text. Bathymetry in metres.

Fig. 2. Transmitted light and cathodoluminescence photomicrographs of detrital zircons in (a) BGS borehole 99/2A, 45.65-45.72 m and (b) DSDP Site 555- 88-5, 18-25 cm. Note that the zircons from 99/2A show greater visible structural incoherence, including fractures and zoning, compared with those from Site 555.

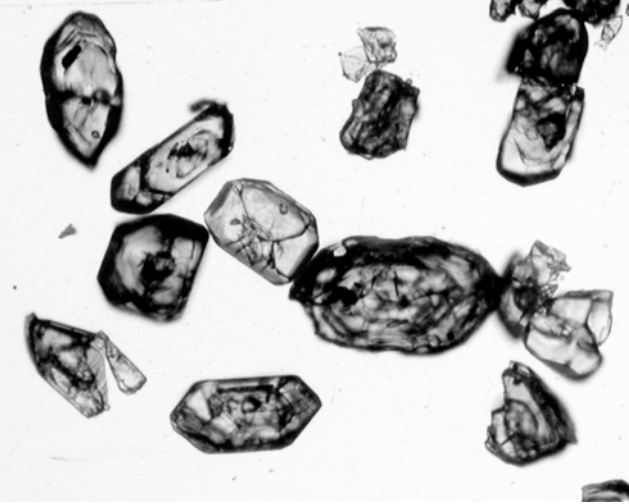
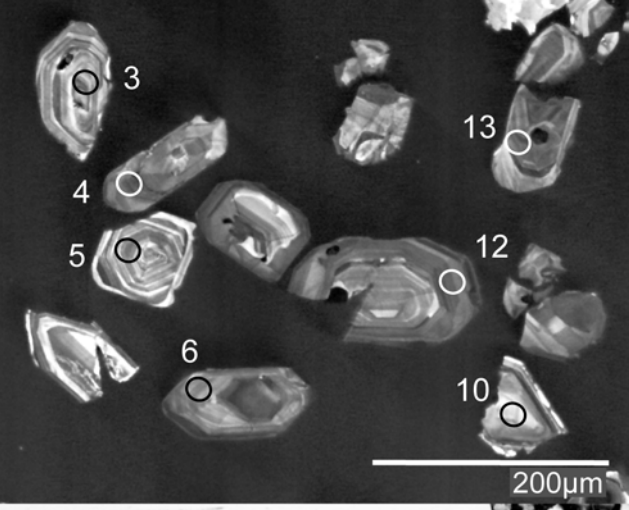
Fig. 3. Detrital zircons from (a) BGS borehole 99/2A, 45.65-45.72 m, and (b) DSDP Site 555- 88-5, 18-25 cm, plotted on  $^{206}\text{Pb}/^{238}\text{U} - ^{207}\text{Pb}/^{235}\text{U}$  diagrams. Error ellipses are  $1\sigma$ . Many of the grains in BGS borehole 99/2A are discordant, with the U-Pb isotopic data defining a simple discordia line. A linear regression of the zircon age data forced through a lower intercept at 55 Ma is shown in (a). By contrast, the zircons from DSDP Site 555 are mostly concordant.

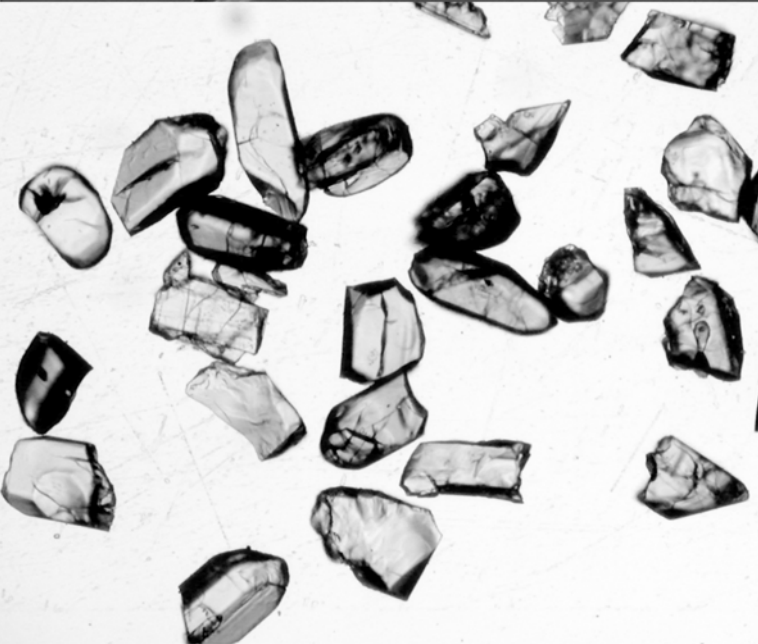
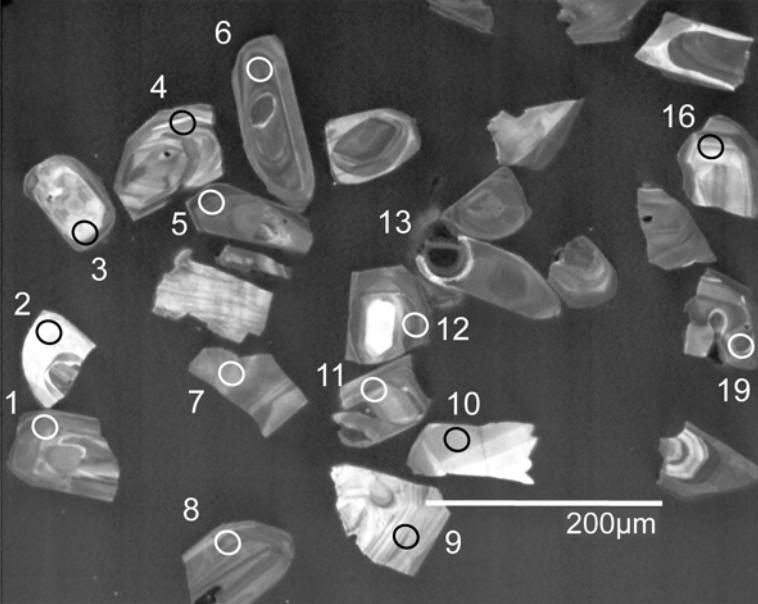
Fig. 4. Combined histogram-relative probability plots of detrital zircon ages from (a) BGS borehole 99/2A, 45.65-45.72 m and (b) DSDP Site 555-88-5, 18-25 cm. Analyses more than 20% discordant have been excluded from the plots. Note that the plot for Site 555 does not show two younger zircons dated as c. 1005 Ma and c. 1110 Ma.

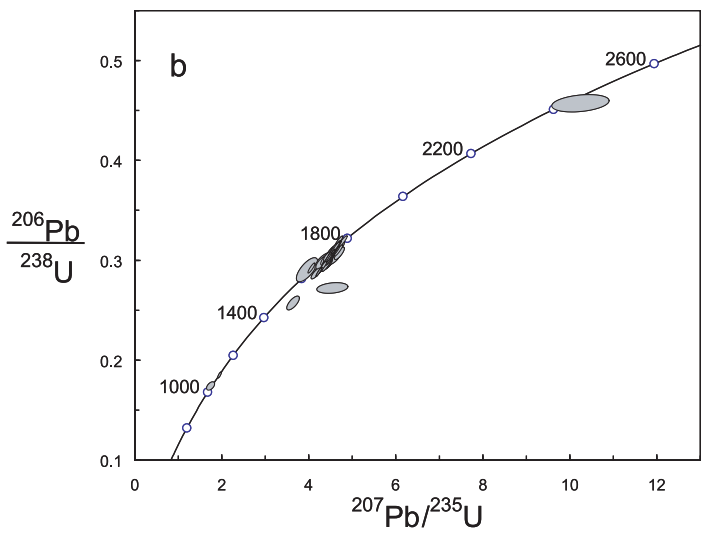
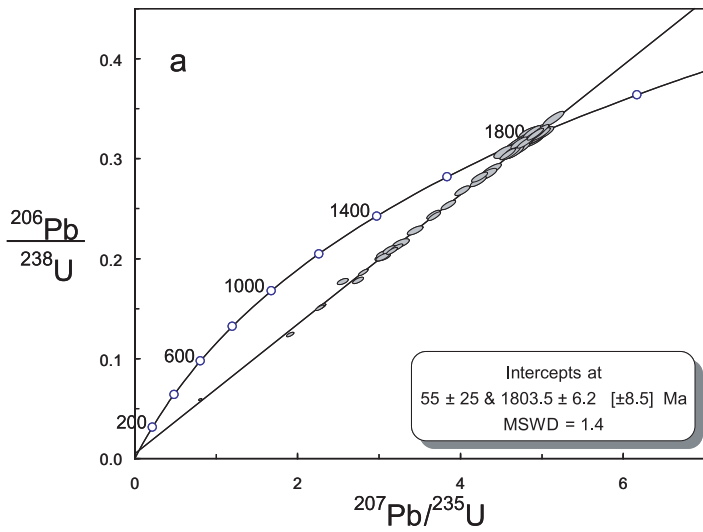
Fig. 5. U-Pb crystallisation ages vs. initial  $\epsilon_{\text{Hf}}$  for BGS borehole 99/2A, 45.65-45.72 m and DSDP Site 555-88-5, 18-25 cm. CHUR = Chondritic Uniform Reservoir. DM = Depleted Mantle

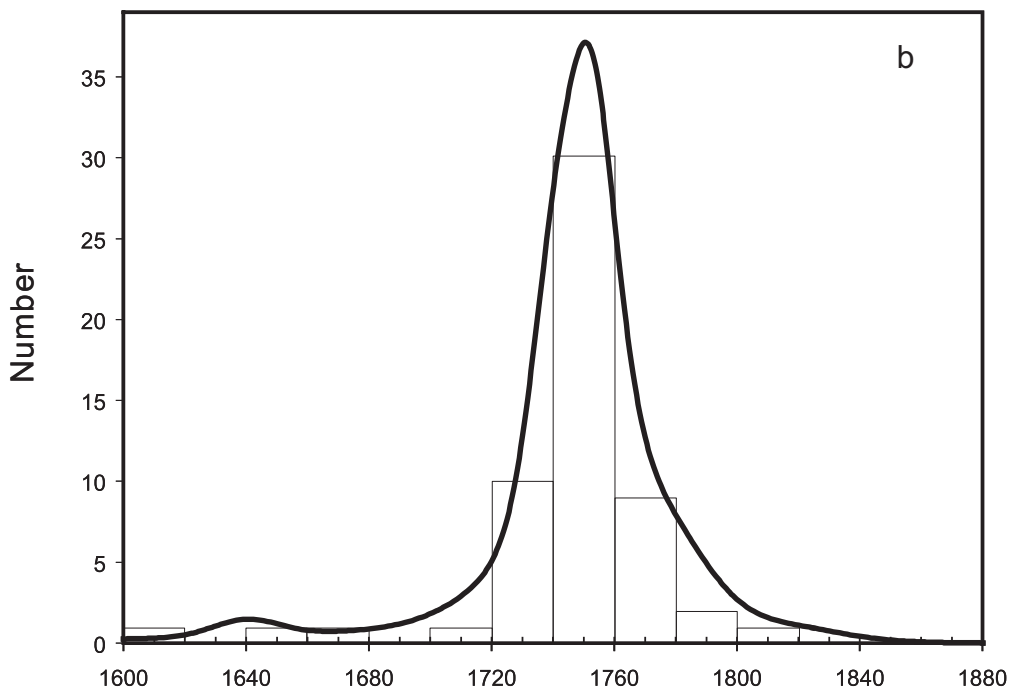
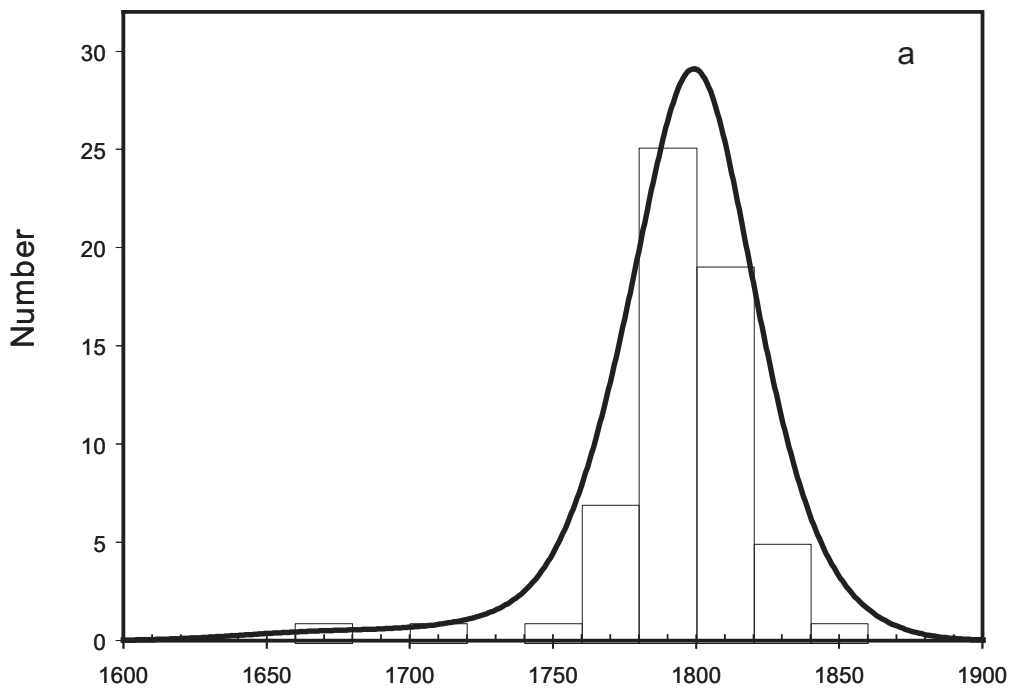
Fig. 6. Comparison of U-Pb ages from the sites on Edoras Bank and Hatton Bank with the available U-Pb zircon crystallisation ages from the Ketilidian Belt of southern Greenland (from Garde et al., 2002), Rockall Bank and the Annagh Gneiss (from Daly et al., 1995 and Scanlon and Daly, 2001), Stanton Bank (Scanlon et al., 2003), Islay (Marcantonio et al., 1988) and Inishtrahull (Daly et al., 1991). The ages are shown on a pre-drift reconstruction of the southern NE Atlantic region, adapted from Cole and Peachey (1999), showing the location of major terrane boundaries. The position of the Archaean-Palaeoproterozoic boundary across the northern part of the Rockall Plateau is adapted from Dickin (1992), Dickin and Durant (2002) and Kimbell et al. (2005).

KB = Ketilidian Belt, NAC = North Atlantic Craton, B = Blackstones Bank, SB = Stanton Bank. A, C, D = samples with U-Pb ages from Rockall Bank.





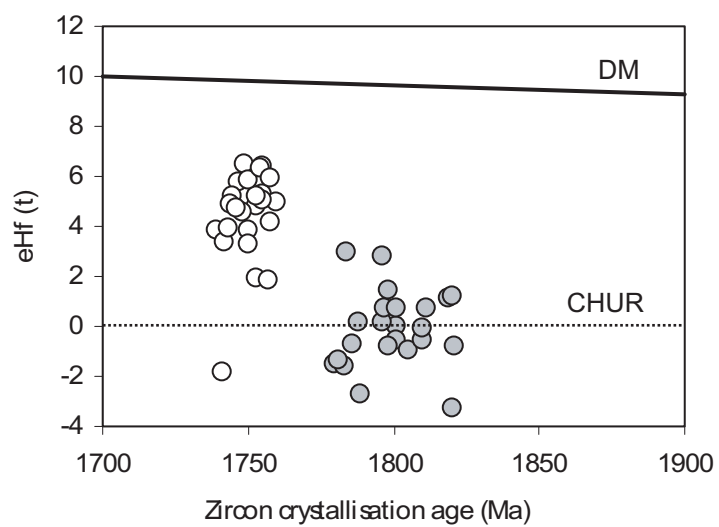




$^{207}\text{Pb}/^{206}\text{Pb}$  Age (Ma)

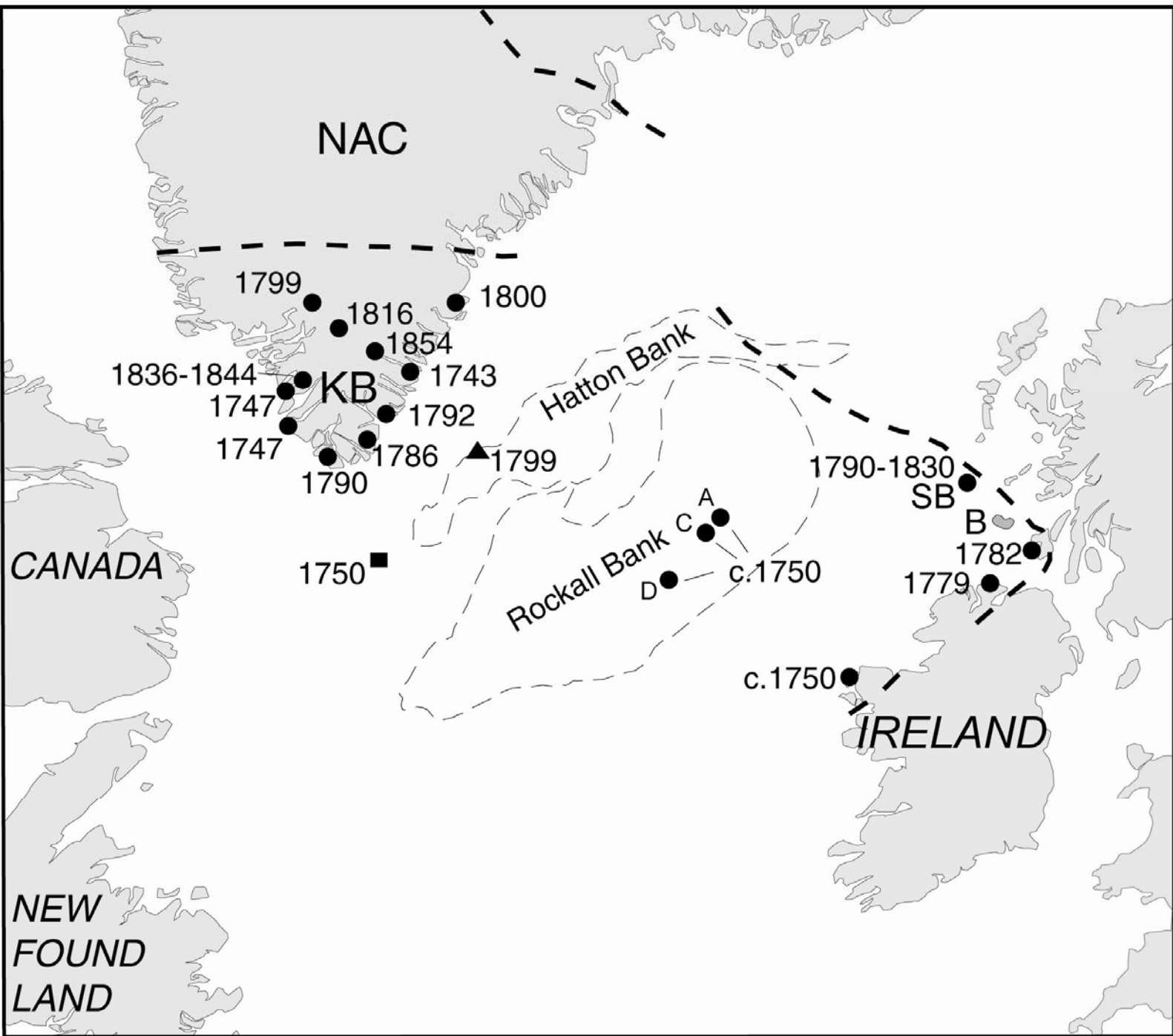
Relative probability

Relative probability



○ DSDP Site 555

● BGS Borehole 99/2A



--- Terrane boundary

 Approximate location of Hatton Bank and Rockall Bank microcontinents

● Previously dated basement samples (age in Ma)

▲ Detrital age from Borehole 99/2A

■ Detrital age from Site 555

Table 1. Summary of SHRIMP U-Pb zircon results for BGS borehole 99/2A, 45.65-45.72 m (Hatton Bank). Uncertainties given at the one  $\sigma$  level. Error in FC1 Reference zircon calibration was 0.37% for the analytical session (not included in above errors but required when comparing  $^{206}\text{Pb}/^{238}\text{U}$  data from different mounts).  $f_{206}$  % denotes the percentage of  $^{206}\text{Pb}$  that is common Pb. Correction for common Pb made using the measured  $^{204}\text{Pb}/^{206}\text{Pb}$  ratio. For % Disc, 0% denotes a concordant analysis.

Grain. spot	U (ppm)	Th (ppm)	Pb* (ppm)	$^{204}\text{Pb}/^{206}\text{Pb}$	$f_{206}$ %	Total Ratios				Radiogenic Ratios				$\rho$	Age (Ma)							
						$^{238}\text{U}/^{206}\text{Pb}$	$\pm$	$^{207}\text{Pb}/^{206}\text{Pb}$	$\pm$	$^{206}\text{Pb}/^{238}\text{U}$	$\pm$	$^{207}\text{Pb}/^{235}\text{U}$	$\pm$		$^{206}\text{Pb}/^{238}\text{U}$	$\pm$	$^{207}\text{Pb}/^{206}\text{Pb}$	$\pm$	% Disc			
1.1	289	180	0.62	68.7	0.000128	0.20	3.615	0.046	0.1122	0.0008	0.2761	0.0035	4.205	0.066	0.1105	0.0010	0.818	1572	18	1807	16	13
2.1	191	90	0.47	51.5	0.000052	0.08	3.189	0.044	0.1108	0.0010	0.3133	0.0043	4.756	0.079	0.1101	0.0010	0.828	1757	21	1801	17	2
3.1	348	246	0.71	60.1	0.000471	0.73	4.966	0.062	0.1164	0.0011	0.1999	0.0025	3.031	0.062	0.1100	0.0018	0.605	1175	13	1799	30	35
4.1	880	461	0.52	133.4	0.000453	0.71	5.669	0.063	0.1114	0.0009	0.1751	0.0019	2.542	0.045	0.1053	0.0015	0.620	1040	11	1719	26	39
5.1	272	143	0.53	48.6	0.000167	0.26	4.813	0.061	0.1114	0.0009	0.2072	0.0026	3.119	0.056	0.1092	0.0014	0.712	1214	14	1785	23	32
6.1	228	94	0.41	56.5	0.000051	0.08	3.471	0.050	0.1107	0.0011	0.2879	0.0042	4.366	0.077	0.1100	0.0011	0.823	1631	21	1799	18	9
7.1	80	52	0.65	21.7	0.000086	0.13	3.159	0.056	0.1097	0.0014	0.3162	0.0056	4.732	0.104	0.1086	0.0014	0.798	1771	27	1775	24	0
8.1	289	113	0.39	80.6	0.000041	0.06	3.084	0.039	0.1118	0.0008	0.3241	0.0042	4.969	0.075	0.1112	0.0009	0.846	1810	20	1819	15	1
9.1	159	78	0.49	41.7	0.000239	0.37	3.266	0.048	0.1127	0.0011	0.3050	0.0045	4.603	0.094	0.1094	0.0015	0.722	1716	22	1790	26	4
10.1	239	106	0.44	63.1	0.000294	0.46	3.256	0.045	0.1114	0.0010	0.3057	0.0042	4.528	0.089	0.1074	0.0015	0.705	1719	21	1756	26	2
11.1	169	66	0.39	46.2	0.000089	0.14	3.146	0.046	0.1125	0.0011	0.3174	0.0046	4.872	0.091	0.1113	0.0013	0.781	1777	23	1821	21	2
12.1	349	198	0.57	61.3	0.000384	0.60	4.894	0.062	0.1140	0.0009	0.2031	0.0026	3.047	0.061	0.1088	0.0017	0.638	1192	14	1779	28	33
13.1	537	249	0.46	123.6	0.000243	0.38	3.735	0.044	0.1123	0.0007	0.2667	0.0031	4.007	0.061	0.1090	0.0011	0.771	1524	16	1782	18	14
14.1	187	112	0.60	52.4	0.000137	0.21	3.072	0.043	0.1131	0.0010	0.3249	0.0046	4.983	0.088	0.1112	0.0012	0.796	1813	22	1820	19	0
15.1	296	131	0.44	51.0	0.000192	0.30	4.984	0.063	0.1124	0.0009	0.2000	0.0026	3.030	0.053	0.1098	0.0013	0.725	1176	14	1797	22	35
16.1	142	69	0.49	38.5	0.000188	0.29	3.168	0.048	0.1112	0.0011	0.3148	0.0048	4.715	0.100	0.1086	0.0016	0.713	1764	23	1777	27	1
17.1	450	260	0.58	94.0	0.000139	0.22	4.111	0.049	0.1111	0.0007	0.2427	0.0029	3.656	0.054	0.1092	0.0010	0.803	1401	15	1787	16	22
18.1	192	126	0.66	53.1	0.000069	0.11	3.102	0.043	0.1103	0.0009	0.3220	0.0044	4.855	0.083	0.1094	0.0011	0.808	1799	22	1789	18	-1
19.1	157	71	0.45	43.0	0.000104	0.16	3.132	0.045	0.1106	0.0016	0.3188	0.0046	4.800	0.104	0.1092	0.0018	0.668	1784	23	1786	29	0
20.1	147	98	0.67	40.6	0.000119	0.19	3.108	0.046	0.1129	0.0011	0.3211	0.0047	4.929	0.091	0.1113	0.0012	0.803	1795	23	1821	20	1
21.1	290	211	0.73	80.4	0.000000	0.00	3.096	0.040	0.1101	0.0008	0.3230	0.0042	4.905	0.073	0.1101	0.0008	0.869	1805	20	1801	13	0
22.1	128	60	0.47	35.1	0.000086	0.13	3.142	0.048	0.1110	0.0012	0.3178	0.0049	4.812	0.096	0.1098	0.0014	0.770	1779	24	1796	23	1
23.1	342	184	0.54	92.6	0.000022	0.03	3.168	0.039	0.1101	0.0007	0.3155	0.0039	4.779	0.067	0.1098	0.0007	0.882	1768	19	1797	12	2
24.1	3282	2985	0.91	160.3	0.000638	1.01	17.592	0.186	0.1111	0.0006	0.0563	0.0006	0.794	0.015	0.1024	0.0016	0.571	353	4	1668	28	79
25.1	126	71	0.57	33.8	0.000209	0.33	3.191	0.049	0.1117	0.0014	0.3123	0.0048	4.687	0.105	0.1088	0.0018	0.683	1752	24	1780	30	2
26.1	134	70	0.52	37.1	0.000150	0.23	3.106	0.054	0.1119	0.0012	0.3212	0.0055	4.866	0.107	0.1099	0.0015	0.785	1795	27	1798	25	0
27.1	142	60	0.42	39.6	0.000000	0.00	3.072	0.046	0.1090	0.0011	0.3255	0.0049	4.892	0.089	0.1090	0.0011	0.829	1817	24	1783	19	-2
28.1	235	101	0.43	65.2	0.000016	0.03	3.097	0.041	0.1109	0.0009	0.3229	0.0043	4.928	0.077	0.1107	0.0009	0.854	1804	21	1811	15	0
29.1	248	151	0.61	68.7	0.000011	0.02	3.105	0.045	0.1092	0.0009	0.3220	0.0047	4.842	0.080	0.1091	0.0009	0.877	1800	23	1784	15	-1
30.1	244	129	0.53	65.6	0.000057	0.09	3.193	0.046	0.1111	0.0009	0.3129	0.0045	4.760	0.079	0.1103	0.0009	0.864	1755	22	1805	15	3
31.1	394	227	0.58	60.0	0.000212	0.33	5.651	0.069	0.1151	0.0009	0.1764	0.0022	2.730	0.046	0.1123	0.0013	0.728	1047	12	1836	21	43
32.1	226	162	0.72	60.1	0.000084	0.13	3.231	0.043	0.1118	0.0009	0.3091	0.0041	4.715	0.078	0.1106	0.0011	0.809	1736	20	1810	18	4
33.1	305	146	0.48	80.2	0.000154	0.24	3.271	0.041	0.1126	0.0008	0.3050	0.0039	4.646	0.072	0.1105	0.0010	0.814	1716	19	1808	16	5
34.1	694	295	0.43	89.8	0.000251	0.39	6.639	0.076	0.1136	0.0007	0.1500	0.0017	2.279	0.035	0.1102	0.0011	0.744	901	10	1802	19	50
35.1	184	81	0.44	49.0	0.000191	0.30	3.229	0.051	0.1111	0.0010	0.3088	0.0049	4.622	0.094	0.1086	0.0014	0.770	1735	24	1775	24	2
36.1	740	469	0.63	77.7	0.000281	0.44	8.182	0.095	0.1168	0.0008	0.1217	0.0014	1.895	0.030	0.1130	0.0013	0.721	740	8	1847	20	60
37.1	376	123	0.33	98.4	0.000034	0.05	3.285	0.043	0.1105	0.0007	0.3043	0.0040	4.615	0.068	0.1100	0.0007	0.893	1712	20	1800	12	5
38.1	261	94	0.36	76.0	0.000042	0.07	2.947	0.041	0.1102	0.0008	0.3391	0.0048	5.127	0.085	0.1096	0.0009	0.854	1882	23	1794	16	-5
39.1	432	158	0.37	112.6	0.000057	0.09	3.291	0.039	0.1099	0.0007	0.3036	0.0036	4.568	0.062	0.1091	0.0007	0.874	1709	18	1785	12	4
40.1	192	135	0.71	35.2	0.000129	0.20	4.675	0.064	0.1124	0.0014	0.2135	0.0029	3.257	0.068	0.1107	0.0017	0.658	1247	16	1810	29	31
41.1	165	79	0.48	45.7	0.000212	0.33	3.098	0.043	0.1109	0.0010	0.3222	0.0045	4.855	0.081	0.1093	0.0010	0.836	1800	24	1788	17	-1
42.1	319	175	0.55	69.2	0.000093	0.15	3.958	0.049	0.1116	0.0008	0.2523	0.0031	3.838	0.059	0.1103	0.0010	0.802	1450	16	1805	17	20
43.1	140	76	0.54	39.2	0.000445	0.69	3.055	0.044	0.1149	0.0011	0.3251	0.0047	4.881	0.117	0.1089	0.0021	0.609	1815	23	1781	35	-2
44.1	825	378	0.46	105.8	0.000205	0.32	6.700	0.078	0.1131	0.0006	0.1488	0.0017	2.262	0.033	0.1103	0.0009	0.806	894	10	1804	16	50
45.1	221	103	0.47	61.8	0.000059	0.09	3.069	0.040	0.1091	0.0008	0.3255	0.0042	4.861	0.076	0.1083	0.0009	0.835	1817	21	1771	16	-3
46.1	192	86	0.45	46.7	0.000079	0.12	3.525	0.048	0.1115	0.0012	0.2833	0.0039	4.314	0.077	0.1104	0.0013	0.764	1608	19	1807	21	11
47.1	440	250	0.57	91.1	0.000137	0.21	4.144	0.048	0.1122	0.0006	0.2408	0.0028	3.663	0.051	0.1103	0.0008	0.833	1391	14	1805	14	23
48.1	290	162	0.56	70.1	0.000086	0.13	3.562	0.043	0.1103	0.0007	0.2804	0.0034	4.217	0.064	0.1091	0.0010	0.806	1593	17	1784	16	11
49.1	284	199	0.70	78.9	0.000029	0.05	3.090	0.037	0.1103	0.0007	0.3235	0.0039	4.903	0.067	0.1099	0.0007	0.885	1807	19	1798	12	0
50.1	281	97	0.34	79.1	0.000020	0.03	3.055	0.037	0.1104	0.0007	0.3273	0.0040	4.969	0.068	0.1101	0.0007	0.883	1825	19	1801	12	-1
51.1	258	133	0.51	70.0	0.000063	0.10	3.172	0.039	0.1091	0.0007	0.3150	0.0039	4.702	0.068	0.1083	0.0008	0.851	1765	19	1771	14	0
52.1	173	68	0.39	33.8	0.000130	0.20	4.401	0.058	0.1115	0.0010	0.2268	0.0030	3.432	0.063	0.1098	0.0014	0.726	1318	16	1795	23	27
53.1	266	137	0.52	70.3	0																	

Table 2. Summary of SHRIMP U-Pb zircon results for DSDP sample 555-88-5, 18-25 cm (Edoras Bank). Uncertainties given at the one  $\sigma$  level. Error in FC1 Reference zircon calibration was 0.37% for the analytical session (not included in above errors but required when comparing  $^{206}\text{Pb}/^{238}\text{U}$  data from different mounts).  $f_{206}$  % denotes the percentage of  $^{206}\text{Pb}$  that is common Pb. Correction for common Pb made using the measured  $^{204}\text{Pb}/^{206}\text{Pb}$  ratio. For % Disc, 0% denotes a concordant analysis.

Grain. spot	U (ppm)	Th (ppm)	Pb* (ppm)	$^{204}\text{Pb}/^{206}\text{Pb}$	$f_{206}$ %	Total Ratios				Radiogenic Ratios				$\rho$	Age (Ma)							
						$^{238}\text{U}/^{206}\text{Pb}$	$\pm$	$^{207}\text{Pb}/^{206}\text{Pb}$	$\pm$	$^{206}\text{Pb}/^{238}\text{U}$	$\pm$	$^{207}\text{Pb}/^{235}\text{U}$	$\pm$		$^{206}\text{Pb}/^{238}\text{U}$	$\pm$	$^{207}\text{Pb}/^{206}\text{Pb}$	$\pm$	% Disc			
1.1	615	142	0.23	158.6	0.000059	0.09	3.329	0.042	0.1081	0.0011	0.3001	0.0038	4.440	0.073	0.1073	0.0011	0.773	1692	19	1754	19	4
2.1	172	74	0.43	44.3	0.000458	0.72	3.343	0.071	0.1125	0.0015	0.2969	0.0064	4.352	0.155	0.1063	0.0030	0.601	1676	32	1737	52	3
3.1	273	67	0.24	69.4	0.000382	0.60	3.374	0.054	0.1125	0.0012	0.2946	0.0047	4.360	0.108	0.1073	0.0020	0.648	1665	23	1754	34	5
4.1	375	73	0.19	95.9	0.000289	0.46	3.362	0.051	0.1088	0.0011	0.2961	0.0045	4.279	0.095	0.1048	0.0017	0.680	1672	22	1711	30	2
5.1	685	125	0.18	159.5	0.000145	0.22	3.689	0.049	0.1229	0.0060	0.2705	0.0036	4.511	0.232	0.1210	0.0060	0.259	1543	18	1971	89	22
6.1	715	160	0.22	183.7	0.000047	0.07	3.345	0.040	0.1087	0.0006	0.2987	0.0036	4.452	0.060	0.1081	0.0007	0.888	1685	18	1768	11	5
7.1	423	128	0.30	108.0	0.000058	0.09	3.360	0.048	0.1090	0.0008	0.2973	0.0042	4.437	0.073	0.1082	0.0009	0.862	1678	21	1770	15	5
8.1	667	132	0.20	174.9	0.000084	0.13	3.277	0.039	0.1073	0.0011	0.3048	0.0036	4.460	0.071	0.1061	0.0011	0.749	1715	18	1734	19	1
9.1	350	109	0.31	89.7	0.000141	0.22	3.350	0.045	0.1088	0.0009	0.2979	0.0040	4.388	0.073	0.1068	0.0011	0.800	1681	20	1746	18	4
10.1	341	117	0.34	89.7	0.000100	0.16	3.270	0.044	0.1124	0.0009	0.3053	0.0041	4.674	0.077	0.1110	0.0011	0.814	1718	20	1817	17	5
11.1	431	125	0.29	110.3	0.000157	0.25	3.360	0.047	0.1103	0.0009	0.2969	0.0042	4.426	0.081	0.1081	0.0013	0.764	1676	21	1768	22	5
12.1	653	64	0.10	256.4	0.000023	0.03	2.187	0.028	0.1623	0.0066	0.4570	0.0058	10.208	0.433	0.1620	0.0066	0.298	2427	26	2477	68	2
13.1	640	122	0.19	167.6	0.000119	0.19	3.278	0.043	0.1090	0.0010	0.3045	0.0040	4.507	0.075	0.1073	0.0011	0.781	1714	20	1755	19	2
14.1	766	72	0.09	208.8	0.000089	0.14	3.151	0.037	0.1087	0.0006	0.3174	0.0037	4.761	0.062	0.1088	0.0006	0.908	1777	19	1779	10	0
15.1	412	85	0.21	110.7	0.000075	0.12	3.200	0.042	0.1095	0.0014	0.3121	0.0041	4.668	0.090	0.1085	0.0015	0.682	1751	20	1774	26	1
16.1	328	86	0.26	86.6	0.000093	0.15	3.255	0.046	0.1076	0.0010	0.3068	0.0043	4.498	0.082	0.1063	0.0012	0.778	1725	21	1737	21	1
17.1	571	117	0.20	150.7	0.000057	0.09	3.251	0.044	0.1069	0.0007	0.3073	0.0041	4.498	0.070	0.1062	0.0008	0.870	1727	20	1734	14	0
18.1	225	93	0.41	58.4	0.000139	0.22	3.318	0.051	0.1077	0.0011	0.3008	0.0047	4.389	0.083	0.1058	0.0012	0.814	1695	23	1729	20	2
19.1	177	89	0.50	46.1	0.000133	0.21	3.308	0.055	0.1112	0.0013	0.3016	0.0050	4.549	0.111	0.1094	0.0019	0.687	1699	25	1789	32	5
20.1	1272	340	0.27	335.9	0.000029	0.05	3.252	0.036	0.1080	0.0004	0.3073	0.0034	4.562	0.054	0.1077	0.0004	0.944	1728	17	1760	7	2
21.1	545	116	0.21	141.8	0.000010	0.01	3.304	0.039	0.1071	0.0006	0.3026	0.0036	4.464	0.058	0.1070	0.0006	0.898	1704	18	1749	11	3
22.1	967	222	0.23	255.6	0.000007	0.01	3.251	0.036	0.1065	0.0004	0.3075	0.0034	4.510	0.053	0.1064	0.0004	0.933	1729	17	1738	8	1
23.1	540	128	0.24	135.9	0.000021	0.03	3.415	0.043	0.1089	0.0006	0.2927	0.0037	4.384	0.061	0.1086	0.0006	0.908	1655	18	1777	11	7
24.1	576	111	0.19	152.5	0.000007	0.01	3.244	0.041	0.1096	0.0006	0.3083	0.0039	4.654	0.064	0.1095	0.0006	0.912	1732	19	1791	10	3
25.1	455	181	0.40	117.8	-	<0.01	3.316	0.036	0.1065	0.0005	0.3016	0.0033	4.429	0.052	0.1065	0.0005	0.931	1699	16	1741	8	2
26.1	458	121	0.26	119.4	0.000005	0.01	3.299	0.036	0.1075	0.0005	0.3031	0.0033	4.487	0.053	0.1074	0.0005	0.932	1707	16	1755	8	3
27.1	818	242	0.30	214.2	-	<0.01	3.280	0.035	0.1071	0.0003	0.3049	0.0032	4.508	0.050	0.1072	0.0003	0.957	1716	16	1753	6	2
28.1	887	194	0.22	229.5	0.000001	0.00	3.322	0.035	0.1073	0.0003	0.3010	0.0032	4.451	0.049	0.1072	0.0003	0.960	1696	16	1753	6	3
29.1	59	57	0.96	8.8	0.000113	0.19	5.811	0.097	0.0742	0.0014	0.1718	0.0029	1.719	0.056	0.0726	0.0020	0.520	1022	16	1003	56	-2
30.1	306	74	0.24	80.4	0.000001	0.00	3.270	0.037	0.1075	0.0006	0.3058	0.0035	4.532	0.057	0.1075	0.0006	0.909	1720	17	1757	10	0
31.1	413	82	0.20	111.0	0.000004	0.01	3.197	0.035	0.1071	0.0005	0.3128	0.0035	4.619	0.055	0.1071	0.0005	0.929	1755	17	1750	8	0
32.1	641	161	0.25	172.5	0.000019	0.03	3.195	0.034	0.1076	0.0004	0.3129	0.0033	4.632	0.053	0.1074	0.0004	0.943	1755	16	1755	7	0
33.1	363	227	0.62	97.4	0.000006	0.01	3.201	0.036	0.1076	0.0005	0.3123	0.0035	4.631	0.056	0.1075	0.0005	0.919	1752	17	1758	9	0
34.1	165	73	0.44	42.2	0.000000	0.00	3.359	0.042	0.1071	0.0008	0.2977	0.0037	4.398	0.064	0.1071	0.0008	0.860	1680	19	1751	14	4
35.1	673	158	0.23	165.8	0.000003	0.01	3.488	0.037	0.1066	0.0004	0.2866	0.0031	4.210	0.048	0.1065	0.0004	0.945	1625	15	1741	7	7
36.1	303	80	0.26	79.5	0.000027	0.04	3.273	0.037	0.1073	0.0006	0.3054	0.0035	4.502	0.057	0.1069	0.0006	0.898	1718	17	1747	10	2
37.1	398	227	0.57	104.4	-	<0.01	3.273	0.036	0.1070	0.0005	0.3055	0.0034	4.517	0.054	0.1072	0.0005	0.921	1719	17	1753	9	2
38.1	690	138	0.20	185.1	0.000006	0.01	3.202	0.034	0.1071	0.0004	0.3123	0.0033	4.610	0.052	0.1071	0.0004	0.946	1752	16	1750	7	0
39.1	237	66	0.28	37.2	-	<0.01	5.478	0.066	0.0760	0.0007	0.1827	0.0022	1.931	0.029	0.0766	0.0007	0.810	1082	12	1112	17	3
40.1	278	115	0.41	69.3	-	<0.01	3.442	0.040	0.1008	0.0006	0.2906	0.0034	4.041	0.052	0.1009	0.0006	0.895	1644	17	1640	11	0
41.1	292	83	0.29	79.7	0.000018	0.03	3.151	0.036	0.1070	0.0006	0.3172	0.0036	4.672	0.059	0.1068	0.0006	0.908	1776	18	1745	10	-2
42.1	407	92	0.23	108.2	0.000008	0.01	3.227	0.036	0.1065	0.0005	0.3098	0.0034	4.545	0.055	0.1064	0.0005	0.923	1740	17	1739	9	0
43.1	281	88	0.31	73.3	0.000030	0.05	3.292	0.038	0.1070	0.0006	0.3036	0.0035	4.461	0.058	0.1066	0.0006	0.899	1709	17	1742	10	2
44.1	469	179	0.38	124.4	0.000018	0.03	3.242	0.036	0.1073	0.0005	0.3083	0.0034	4.552	0.054	0.1071	0.0005	0.931	1733	17	1750	8	1
45.1	704	186	0.26	186.2	0.000007	0.01	3.250	0.036	0.1074	0.0004	0.3077	0.0034	4.552	0.053	0.1073	0.0004	0.950	1729	17	1754	7	1
46.1	782	166	0.21	193.0	0.000004	0.01	3.483	0.037	0.1064	0.0004	0.2871	0.0031	4.211	0.047	0.1064	0.0004	0.950	1627	15	1738	6	6
47.1	17	3	0.21	4.1	0.000671	1.09	3.450	0.096	0.1020	0.0027	0.2888	0.0080	3.941	0.153	0.0990	0.0027	0.713	1636	41	1605	51	-2
48.1	541	166	0.31	140.9	0.000135	0.21	3.302	0.036	0.1079	0.0005	0.3022	0.0033	4.422	0.072	0.1061	0.0013	0.681	1702	17	1734	22	2
49.1	547	107	0.19	143.5	-	<0.01	3.274	0.036	0.1066	0.0005	0.3054	0.0034	4.491	0.053	0.1066	0.0005	0.932	1718	17	1743	8	1
50.1	1032	252	0.24	276.4	0.000001	<0.01	3.208	0.034	0.1065	0.0004	0.3119	0.0033	4.600	0.052	0.1070	0.0005	0.928	1750	17	1748	8	0
51.1	492	165	0.33	126.2	0.000022	0.03	3.350	0.040	0.1070	0.0005	0.2984	0.0035	4.391	0.057	0.1067	0.0005	0.918	1683	18	1744	9	3
52.1	502	167	0.33	126.3	0.000014	0.02	3.414	0.038	0.1071	0.0005	0.2928	0.0033	4.315	0.053	0.1069	0.0005	0.913	1656	16	1747	9	5
53.1	59	29	0.48	13.0	0.000091	0.14	3.907	0.070	0.103													

Table 3. Hf isotopic compositions of detrital zircons from BGS borehole 99/2A and DSDP Site 555.  $^{176}\text{Lu}$  decay constant from Soderlund et al. (2004). Chondritic values from Blichert-Toft and Albarède (1997). Present day depleted mantle values from Vervoort and Blichert-Toft (1999). “Bulk Earth” from Goodge and Vervoort (2006).

Sample	Grain	$^{176}\text{Hf}/^{177}\text{Hf}$	$\pm 2\text{ se}$	$^{176}\text{Lu}/^{177}\text{Hf}$	$\pm 2\text{ se}$	U-Pb age (t1)	$\epsilon\text{ Hf}(0)$	$^{176}\text{Hf}/^{177}\text{Hf}_{(t1)}$	$\epsilon\text{ Hf}(t1)$	$T_{\text{DM}}$	
99/2A, 45.65-45.72 m	2	0.281659	0.000050	0.000643	0.000036	1801	-39.35	0.281637	0.02	2417	
	8	0.281700	0.000064	0.001276	0.000117	1819	-37.92	0.281656	1.09	2363	
	11	0.281614	0.000050	0.000383	0.000008	1821	-40.95	0.281601	-0.82	2486	
	14	0.281556	0.000038	0.000699	0.000013	1820	-43.01	0.281532	-3.30	2643	
	18	0.281606	0.000042	0.001096	0.000024	1789	-41.24	0.281569	-2.69	2581	
	19	0.281641	0.000049	0.000427	0.000006	1786	-39.99	0.281627	-0.70	2451	
	21	0.281651	0.000049	0.000901	0.000006	1801	-39.64	0.281620	-0.58	2456	
	22	0.281659	0.000039	0.000441	0.000005	1796	-39.34	0.281644	0.16	2404	
	23	0.281689	0.000046	0.000860	0.000019	1797	-38.29	0.281660	0.73	2369	
	25	0.281644	0.000042	0.001045	0.000008	1780	-39.90	0.281608	-1.48	2497	
	26	0.281709	0.000046	0.000911	0.000015	1798	-37.58	0.281678	1.40	2327	
	27	0.281618	0.000038	0.000421	0.000011	1783	-40.79	0.281604	-1.56	2504	
	28	0.281669	0.000034	0.000533	0.000003	1811	-39.02	0.281650	0.71	2381	
	29	0.281757	0.000040	0.000765	0.000016	1784	-35.89	0.281731	2.97	2216	
	30	0.281646	0.000041	0.001107	0.000046	1805	-39.83	0.281608	-0.94	2481	
	32	0.281636	0.000033	0.000610	0.000037	1810	-40.17	0.281615	-0.56	2461	
	41	0.281668	0.000038	0.000560	0.000004	1788	-39.03	0.281649	0.15	2399	
	43	0.281630	0.000037	0.000552	0.000006	1781	-40.38	0.281611	-1.35	2489	
	49	0.281646	0.000046	0.000863	0.000070	1798	-39.83	0.281616	-0.79	2467	
	50	0.281685	0.000033	0.000834	0.000030	1801	-38.44	0.281657	0.71	2374	
	57	0.281647	0.000032	0.000531	0.000019	1810	-39.79	0.281629	-0.08	2431	
	58	0.281749	0.000054	0.000889	0.000016	1796	-36.19	0.281718	2.79	2237	
	60	0.281678	0.000042	0.000590	0.000021	1820	-38.67	0.281658	1.19	2357	
	555-88-5, 18-25 cm	13	0.281834	0.000043	0.000609	0.000014	1755	-33.17	0.281814	5.24	2048
		20	0.281839	0.000047	0.001070	0.000017	1760	-32.99	0.281803	4.99	2068
		21	0.281874	0.000079	0.000654	0.000013	1749	-31.74	0.281853	6.49	1964
		25	0.281646	0.000073	0.000692	0.000064	1741	-39.83	0.281623	-1.86	2491
		26	0.281877	0.000064	0.000887	0.000048	1755	-31.65	0.281848	6.44	1971
		27	0.281765	0.000032	0.001307	0.000002	1753	-35.61	0.281721	1.92	2259
		28	0.281831	0.000065	0.000859	0.000002	1753	-33.29	0.281802	4.78	2076
30		0.281752	0.000031	0.001036	0.000026	1757	-36.08	0.281717	1.86	2266	
31		0.281790	0.000043	0.000400	0.000007	1750	-34.74	0.281776	3.80	2137	
32		0.281826	0.000038	0.000514	0.000004	1755	-33.45	0.281809	5.07	2059	
33		0.281821	0.000074	0.001153	0.000037	1758	-33.65	0.281782	4.19	2118	
36		0.281857	0.000042	0.000719	0.000009	1747	-32.35	0.281833	5.76	2009	
37		0.281828	0.000041	0.000418	0.000012	1753	-33.37	0.281815	5.22	2048	
38		0.281787	0.000041	0.000799	0.000014	1750	-34.82	0.281761	3.25	2172	
41		0.281841	0.000053	0.000636	0.000030	1745	-32.94	0.281819	5.22	2042	
42		0.281796	0.000036	0.000310	0.000007	1739	-34.52	0.281786	3.88	2123	
43		0.281780	0.000041	0.000345	0.000004	1742	-35.08	0.281769	3.34	2160	
44		0.281870	0.000058	0.001085	0.000029	1750	-31.89	0.281834	5.86	2005	
45	0.281870	0.000038	0.000767	0.000005	1754	-31.89	0.281845	6.32	1978		
49	0.281824	0.000041	0.001195	0.000039	1743	-33.53	0.281784	3.92	2124		
50	0.281825	0.000053	0.000808	0.000029	1748	-33.48	0.281799	4.54	2088		
51	0.281829	0.000043	0.000589	0.000008	1744	-33.34	0.281810	4.84	2065		
57	0.281848	0.000048	0.000530	0.000008	1758	-32.69	0.281830	5.88	2009		
58	0.281828	0.000045	0.000713	0.000019	1746	-33.37	0.281805	4.71	2075		